sences, it does not have the cubic symmetry that the intensity measurements indicated. It also requires a 3.0-Å contact distance between NH_4^+ ions at N(2) and N(4) in half of the large cavities. To preserve the cubic symmetry and to avoid the short intercationic approach, we must assume some disorder of the NH_4^+ ions.

It has been assumed that all exchangeable cations in this structure are NH_4^+, none H_3O^+.[8] The high pH during ion exchange and the high stability of NH_4^+ relative to H_3O^+ support this assumption, that all exchangeable cations (except for much less than 1 out of 12) in the solvated crystal where NH_4^+ and that desolvation at 25 °C removed only excess NH_3 (If present) and H_2O; that is, NH_4^+ did not hydrolyze to any significant extent to form H_3O^+ and NH_3 vapor (the pK for this hydrolysis would be 9.26 at 25 °C in aqueous solution). This experiment is not able to distinguish between N and O.

Acknowledgment. This work was supported by the National Science Foundation (Grant No. CHE77-12495). We are indebted to the University of Hawaii Computing Center. L.B.M. gratefully acknowledges a research fellowship from the U.H. Chemistry Department.

Supplementary Material Available: A listing of the observed and calculated structure factors (5 pages). Ordering information is given on any current masthead page.

Characterization of Apical Copper(II)–Thioether Bonding. Structure and Electronic Spectra of Bis(2,2-bis(5-phenyl-2-imidazolyl)propane)copper(II) Diperchlorate and Bis(1,3-bis(5-phenyl-2-imidazolyl)-2-thiopropane)copper(II) Diperchlorate

Hans J. Prochaska,[1a] William F. Schwindinger,[1a] Michael Schwartz,[1a] Mark J. Burk,[1a] Ernest Bernarducci,[1a] Roger A. Lalancette,[1b] Joseph A. Potenza,*[1a] and Harvey J. Schugar*[1a]

Contribution from the Departments of Chemistry, Rutgers, The State University of New Jersey, New Brunswick, New Jersey 08903, and Newark, New Jersey 07102. *Received October 20, 1980*

Abstract: The crystal and molecular structures of bis(2,2-bis(5-phenyl-2-imidazolyl)propane)copper(II) diperchlorate tetramethanolate (**1**) and bis(1,3-bis(5-phenyl-2-imidazolyl)-2-thiopropane)copper(II) diperchlorate pentamethanolate (**2**) have been determined from single-crystal, three-dimensional X-ray data collected by counter methods. Complex **1** crystallized from CH_3OH as light brown prisms in space group $P\bar{1}$ with $Z = 1$, $a = 11.064$ (5) Å, $b = 13.469$ (7) Å, $c = 9.018$ (3) Å, $\alpha = 105.85$ (4)°, $\beta = 104.85$ (4)°, $\gamma = 85.58$ (4)°, $d_{calcd} = 1.393$ g/cm^3, and $d_{obsd} = 1.43$ (5) g/cm^3. Least-squares refinement of 2411 reflections having $F_o^2 > 3\sigma(F_o^2)$ gave a conventional R factor of 0.064. The structure contains discrete Cu(II) monomers having planar N_4 ligand donor sets with Cu–N bond distances of 1.979 (5) and 1.960 (4) Å. The ClO_4^- and CH_3OH groups are lattice species well removed from the copper atoms. Complex **2** crystallized from CH_3OH as orange-brown prisms in space group $P2_1/c$ with $Z = 2$, $a = 12.08$ (2) Å, $b = 11.98$ (2) Å, $c = 18.93$ (3) Å, $\beta = 96.19$ (4)°, $d_{calcd} = 1.360$ g/cm^3, and $d_{obsd} = 1.43$ (5) g/cm^3. Least-squares refinement of 2351 reflections having $F_o^2 \geq 3\sigma(F_o^2)$ gave a conventional R factor of 0.089. The structure contains discrete Cu(II) monomers having tetragonal N_4S_2 ligand donor sets with equatorial Cu–N bond distances of 2.020 (9) and 2.019 (7) Å and apical Cu–S bond distances of 2.824 (5) Å. Electronic and ESR spectra are reported for **1** and **2**. Electronic spectra also are reported for bis(1,2-bis(5-phenyl-2-imidazolyl)ethane)copper(II) diperchlorate (**3**) and bis(1,3-bis(5-*tert*-butyl-2-imidazolyl)-2-thiopropane)copper(II) diperchlorate (**4**). In contrast to the prominant ($\epsilon > 1000$) ligand to metal charge-transfer (LMCT) absorption at ~25 000 cm^{-1} exhibited by equatorial thioether–Cu(II) units (Cu–S = ~2.3 Å), the corresponding absorptions anticipated for complexes **2** and **4** were too weak to detect. Complexes **1–4** all exhibit a weak ($\epsilon \approx 200$) absorption at ~25000 cm^{-1} attributable to poorly resolved π(imidazole) → Cu(II) LMCT. The assignments of thioether → Cu(II) LMCT proposed for plastocyanin and other type 1 copper proteins are reconsidered in view of the above spectroscopic results and the available protein crystallographic data.

The peculiar coordination structures and properties of the Cu(II) sites in the type 1 proteins now are fairly well-defined. Crystallographic studies at ~3 Å resolution of azurin[2] and plastocyanin[3] have shown that the Cu(II) in both proteins is ligated by a distorted tetrahedral arrangement of two imidazole (ImH) nitrogens (N), a cysteine sulfur (S), and a methionine sulfur (S*) atom. Further study of plastocyanin at ~1.6 Å resolution[4] has revealed that the Cu–S* bonding effectively is apical (~2.9 Å); other bond distances within the CuN_2SS^* fragment are normal. Moreover, bond angles within the CuN_2SS^* fragment generally are highly distorted from the ideal 109° value. Detailed electronic spectral studies of azurin, plastocyanin, and stellacyanin recently have been published.[5] Ligand field absorptions of the Cu(II) sites fall in the 5000–11 000 cm^{-1} spectral range. Characteristic absorptions of these proteins at ~13 000 and ~16 000 cm^{-1} convincingly have been assigned to π(S) → Cu(II) and σ(S) → Cu(II)

(1) (a) Rutgers, New Brunswick. (b) Rutgers, Newark.
(2) Adman, E. T.; Stienkamp, R. E.; Sieker, L. C.; Jensen, L. H. *J. Mol. Biol.* **1978**, *123*, 35–47.
(3) Colman, P. M.; Freeman, H. C.; Guss, J. M.; Murata, M.; Norris, V. A.; Ramshaw, J. A. M.; Venkatappa, M. P. *Nature (London)* **1978**, *272*, 319–24.
(4) Private communication, Professor H. C. Freeman.
(5) Solomon, E. I.; Hare, J. W.; Dooley, D. M.; Dawson, J. H.; Stephens, P. J.; Gray, H. B. *J. Am. Chem. Soc.* **1980**, *102*, 168–78.

0002-7863/81/1503-3446$01.25/0

ligand to metal charge transfer (LMCT), respectively. Analogous, but blue-shifted, absorptions are exhibited by a well-characterized model Cu(II)–thiolate chromophore.[6] Finally, a combination of $\sigma(S^*) \rightarrow$ Cu(II) and $\pi(ImH) \rightarrow$ Cu(II) LMCT absorptions are thought to account for protein bands in the 18 000–23 000 cm^{-1} spectral region.[5] Suitable Cu(II) complexes which embody these latter two types of ligation have not been available. In an attempt to model the above $\pi(ImH) \rightarrow$ Cu(II) LMCT, we have shown that tetragonal $Cu(ImH)_4^{2+}$ and $Cu(pyrazole)_4^{2+}$ units exhibit LMCT bands at the same energies[7] and have assigned as π(pyrazole) $\rightarrow$ Cu(II) LMCT the absorptions at 24 700 and 20 200 cm^{-1} which were reported for a fully characterized pseudo-tetrahedral $Cu(pyrazole)_4^{2+}$ complex.[8,9] These absorptions are red-shifted 10 000–12 000 cm^{-1} from their counterparts in tetragonal $Cu(ImH)_4^{2+}$ and $Cu(pyrazole)_4^{2+}$ complexes.[7,10] Our results support the suggestion that $\pi(ImH) \rightarrow$ Cu(II) LMCT bands occur in the 18 000–23 000 cm^{-1} spectral region of the type 1 proteins.[5]

Our purpose in this report is to characterize apical $\sigma(S) \rightarrow$ Cu(II) LMCT absorption. Previous studies have indicated that LMCT absorption associated with apical Cu(II)–Cl bonding (Cu–Cl = ~2.8 Å) is considerably weaker relative to that observed for equatorial Cu–Cl bonding (Cu–Cl = ~2.3 Å).[11] Studies of structurally characterized Cu(II) complexes have indicated that equatorial Cu–thioether bonding (Cu–S* = ~2.3 Å) gives rise to $\sigma(S^*) \rightarrow$ Cu(II) LMCT absorptions at 22 000–26 000 cm^{-1}.[11] We now report the preparation and characterization of complexes **1–4**. Complex **1**, which exhibits apical Cu(II)–thioether bonding,

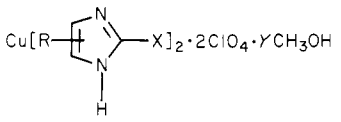

1, X = $\backslash C(CH_3)_2 /$, $Y = 4$, R = phenyl
2, X = $-CH_2SCH_2-$, $Y = 5$, R = phenyl
3, X = $-CH_2CH_2-$, R = phenyl
4, X = $-CH_2SCH_2-$, R = *tert*-butyl

and a spectroscopic reference, complex **2**, have been structurally characterized. Complexes **3** and **4** have been studied spectroscopically but not crystallographically.

Experimental Section

(1) Preparation of Ligands. Ketol esters were prepared from the reaction of various carboxylic acid salts with appropriate α-bromoketones and converted to imidazoles with refluxing $CH_3CH_2CO_2H/NH_4O_2CCH_2CH_3$ mixtures (see Scheme I). Conversions of the ketol esters to imidazoles were more rapid in this mixture than with refluxing $CH_3CO_2H/NH_4O_2CCH_3$[12] and cleaner than with refluxing formamide.[13]

Preparation of 6a. A solution of 6.6 g (0.05 mol) of dimethylmalonic acid (Aldrich Chemical Co.) was neutralized to pH 7.7 with methanolic benzyltrimethylammonium methoxide (Aldrich Chemical Co.) and rotary evaporated to dryness. A solution of this salt (**5a**) and 24 g (0.12 mol) of $PhCH_2C(O)CH_2Br$ (Aldrich Chemical Co.) in 80 mL of $HC(O)NH_2$ was maintained at 25 °C for 20 h and deposited **6a** as a light orange suspension. The product was collected by filtration and washed with H_2O. Two recrystallizations from warm acetone–H_2O mixtures gave 13.8 g (75% yield) of white crystalline **6a**: mp 93–94 °C; ^1H NMR ($CDCl_3$, 60 MHz) δ 1.7 (s, 6 H, CH_3), 5.4 (s, 4 H, CH_2), 7.2–8.0 (m, 10 H, ArH).

Scheme I

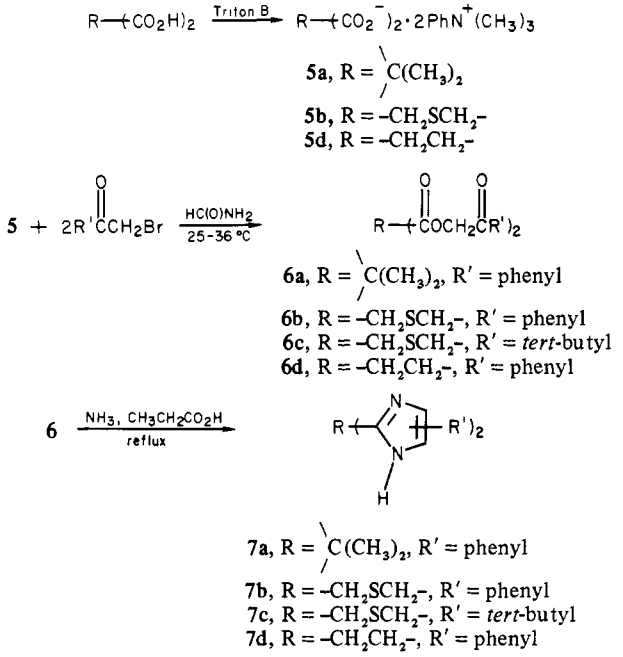

Preparation of 6b. The trityl salt **5b** was formed from 45 g (0.3 mol) of $S(CH_2CO_2H)_2$ (Aldrich Chemical Co.) and reacted with an excess (132 g, 0.66 mol) of $PhCH_2C(O)CH_2Br$ in 450 mL of $HC(O)NH_2$. After being left standing at ~25 °C for 24 h, the orange solution was added to a separatory funnel which contained 150 mL of H_2O and extracted three times with 150-mL portions of $CHCl_3$. The $CHCl_3$ extract was concentrated by rotary evaporation, yielding an orange oil. Addition of 95% ethanol caused the oil to solidify. Two recrystallizations from a minimal amount of boiling 95% ethanol gave 45 g (41% yield) of white crystalline **6b**: mp 96–97 °C; ^1H NMR ($CDCl_3$, 60 MHz) δ 3.7 (s, 4 H, CH_2), 5.5 (s, 4 H, CH_2), 7.4–8.0 (m, 10 H, ArH).

Preparation of 6c. Pinacolone (Aldrich Chemical Co.) was brominated in glacial CH_3CO_2H to 1-bromo-3,3-dimethyl-2-butanone. A solution of 0.13 mol of **6b** (vide supra) and 54.6 g (0.31 mol) of the above bromoketone was stirred at room temperature for 24 h. Dropwise addition of the reaction mixture to 400 mL of H_2O caused crude **6c** to precipitate as a pale yellow solid which melted at 67–68 °C when dried in air (27 g, 58% yield): ^1H NMR ($CDCl_3$, 60 MHz) δ 1.2 (s, 18 H, CH_3), 3.6 (s, 4 H, CH_2), 5.0 (s, 4 H, CH_2). The crude product was sufficiently pure to use without further treatment.

Preparation of 6d. A solution of 23.6 g (0.2 mol) of succinic acid in 150 mL of H_2O was neutralized to pH 7.5 with benzyltrimethylammonium methoxide and reduced in volume to ~50 mL by rotary evaporation. The residue was dissolved in 175 mL of $HC(O)NH_2$ and reacted with 91.6 g (0.46 mol) of $PhCH_2C(O)CH_2Br$ for several hours. Addition of ~50 mL of H_2O followed by cooling to ~10 °C resulted in the precipitation of **6d** as a white powder. The product was collected by filtration, washed with H_2O, and dried in air. The crude product (57 g, 81% yield) melted at 144–146 °C: ^1H NMR ($CDCl_3$, 60 MHz) δ 2.9 (s, 4 H, CH_2), 5.4 (s, 4 H, CH_2), 7.0–8.0 (m, 10 H, ArH). The crude product was subsequently used without further treatment.

Preparation of 7a. A mixture of 13.2 g (0.036 mol) of **6a**, 125 g of $NH_4O_2CCH_2CH_3$, and 180 mL of $CH_3CH_2CO_2H$ was refluxed for 3 h. Slow addition of H_2O and NH_3(aq) (in excess of that required to neutralize the $CH_3CH_2CO_2H$) to the cooled reaction mixture caused precipitation of **7a** as a cream colored solid. The product was collected by filtration, washed with H_2O, dried in air, and triturated with ether. Two recrystallizations from warm CH_3OH/deionized H_2O mixtures gave 4.4 g (37%) of white crystalline **7a**: mp 240–242 °C; ^1H NMR (Me_2SO-d_6, 60 MHz) δ 1.8 (s, 6 H, CH_3), 7.2–8.0 (m, 12 H, ArH).[14] Anal. Calcd for $C_{21}H_{20}N_4$: C, 76.80; H, 6.13; N, 17.06. Found: C, 76.92; H, 6.13; N, 16.89.

Preparation of 7b. After a mixture of 10 g (0.26 mol) of **6b**, 125 g $NH_4O_2CCH_2CH_3$, and 180 mL of $CH_3CH_2CO_2H$ was refluxed for 3 h, propionic acid was removed by rotoevaporation. The residue, a dark oil, was dissolved in $CHCl_3$ and extracted with five 75-mL portions of 5 M

(6) Hughey, J. L., IV; Fawcett, T. G.; Rudich, S. M.; Lalancette, R. A.; Potenza, J. A.; Schugar, H. J. *J. Am. Chem. Soc.* **1979**, *101*, 2617–23.
(7) Bernarducci, E.; Schwindinger, W. F.; Krogh-Jespersen, K.; Schugar, H. J. *J. Am. Chem. Soc.* **1981**, *103*, 1686–91.
(8) Herring, F. G.; Patmore, D. J.; Storr, A. *J. Chem. Soc., Dalton Trans.* **1975**, 711–17.
(9) Patmore, D. J.; Rendle, D. F.; Storr, A.; Trotter, J. *J. Chem. Soc., Dalton Trans.* **1975**, 718–25.
(10) Fawcett, T. G.; Bernarducci, E. E.; Krogh-Jespersen, K.; Schugar, H. J. *J. Am. Chem. Soc.* **1980**, *102*, 2598–2604.
(11) Miskowski, V. M.; Thich, J. A.; Solomon, R.; Schugar, H. J. *J. Am. Chem. Soc.* **1976**, *98*, 8344–50.
(12) Strzybny, P. P. E.; van Es, T.; Backeberg, O. G. *J. Org. Chem.* **1963**, *28*, 3381–91.
(13) Novelli, A.; DeSantis, A. *Tetrahedron Lett.* **1967**, 265–67.
(14) The N–H absorption could not be observed in deuterated Me_2SO.

Table I. Crystal and Refinement Data

	1	2
formula	$Cu[(C_6H_5C_3H_2N_2)_2C(CH_3)_2]_2 \cdot 2ClO_4 \cdot 4CH_3OH$	$Cu[(C_6H_5C_3H_2N_2CH_2)_2S]_2 \cdot 2ClO_4 \cdot 5CH_3OH$
fw	1047.36	1115.56
a, Å	11.064 (5)	12.08 (2)
b, Å	13.469 (7)	11.98 (2)
c, Å	9.018 (3)	18.93 (3)
α, deg	105.85 (4)	90
β, deg	104.85 (4)	96.19 (4)
γ, deg	85.58 (4)	90
space group	$P\bar{1}$	$P2_1/c$
Z	1	2
no. of reflcns used to determine cell constants	15	19
d_{calcd}, g/cm^3	1.385	1.360
d_{obsd}, g/cm^3	1.43 (5)[a]	1.43 (5)[a]
λ(Mo Kα), Å	0.710 69	0.710 69
monochromator	graphite	graphite
linear abs coeff, cm^{-1}	6.34	7.36
crystal dimens, mm	0.15 × 0.42 × 0.52	0.28 × 0.34 × 0.60
abs factor range	1.096–1.315	1.199–1.285
diffractometer	Syntex $P2_1$	Enraf-Nonius CAD-3
data collectn method	θ–2θ	θ–2θ
2θ range, deg	$4 \leq 2\theta \leq 50$	$4 \leq 2\theta < 45$
temp, °C	24 ± 2	24 ± 2
scan rate, deg/min	1.5	10[b]
scan range, deg	$2\theta(K\alpha_1) - 1$ to $2\theta(K\alpha_2) + 1$	$1.2 + 0.7 \tan\theta$
no. std reflcns	3	2
variation in std intens, %	±5	±6
no. unique data collected	4215	3765
no. data used in refinement ($F_o^2 \geq 3\sigma(F_o^2)$)	2411	2351
data:parameter ratio	8.0	7.1
final R_F[c]	0.064	0.089
final R_{wF}[d]	0.067	0.085

[a] Determined by the gradient method using a mixture of CH_3OH and CCl_4. See text for an explanation of the large error limits. [b] Each reflection was scanned twice, and the background on either side was measured for 3 s. This process was repeated up to six times or until 6000 total counts were observed. [c] $R_F = \Sigma||F_o| - |F_c|| / \Sigma|F_o|$. [d] $R_{wF} = (\Sigma w(|F_o| - |F_c|)^2 / \Sigma w F_o^2)^{1/2}$. Unit weights were employed for both structures.

HCl(aq). After the aqueous extract was concentrated to 80 mL, the addition of NH_3(aq) caused **7b** to precipitate as a yellow mass. Two recrystallizations from warm CH_3OH/deionized H_2O mixtures gave 3.8 g (44%) of white crystalline **7b**: mp 226–228 °C (sealed cap); ^{1}H NMR (Me_2SO-d_6, 60 MHz) δ 4.0 (s, 4 H, CH_2), 7.2–8.0 (m, 12 H, ArH).[14] Anal. Calcd for $C_{20}H_{18}N_4S$: C, 69.34; H, 5.24; N, 16.17; S, 9.26. Found: C, 69.11; H, 5.29; N, 16.04; S, 8.54.

Preparation of 7c. A mixture of 2.7 g (8 mmol) of **6c**, 23 g of $NH_4O_2CCH_2CH_3$, and 56 g of $CH_3CH_2CO_2H$ was refluxed for 3 h and added dropwise to a mixture of 700 mL of H_2O and 160 mL of concentrated NH_3(aq). The product separated as a cream colored gum. Three recrystallizations from warm CH_3OH/deionized H_2O mixtures gave 0.7 g (29% yield) of white crystalline **7c**: mp 282–288 °C (sealed cap); ^{1}H NMR (CF_3CO_2D, 60 MHz) δ 1.4 (s, 18 H, CH_3), 4.3 (s, 4 H, CH_2), 7.1 (s, 2 H, ArH).[14] Anal. Calcd for $C_{16}H_{26}N_4S$: C, 62.77; H, 8.55; N, 18.28; S, 10.46. Found: C, 63.09; H, 8.83; N, 18.25; S, 10.53.

Preparation of 7d. A mixture of 10 g (0.028 mol) of **6d**, 100 g of $NH_4O_2CCH_2CH_3$, and 150 mL of $CH_3CH_2CO_2H$ was refluxed for 18 h. A small amount of solid was deposited from the cooled reaction mixture, removed by filtration, and discarded. The propionic acid was removed by rotoevaporation and the residue dissolved in ~70 mL of $CHCl_3$. We intended to extract the product into an aqueous HCl solution. However, addition of 50 mL of 6 M HCl(aq) to the above $CHCl_3$ solution caused the hydrochloride salt of **7d** to precipitate as a white solid. The solid was collected by filtration, triturated with hot $CHCl_3$, and dried in air. Neutralization of an alcohol water solution of the salt with concentrated NH_3(aq) caused **7d** to precipitate as a white powder. Recrystallization from warm alcohol/water gave 3.1 g (36%) of white crystalline **7d**: mp 218–220 °C; ^{1}H NMR (Me_2SO-d_6, 60 MHz) δ 2.4 (m, Me_2SO), 3.1 (s, 4 H, CH_2), 6.7 (br s, 2 H, NH), 7.0–8.0 (m, 12 H, ArH). Anal. Calcd for $C_{20}H_{18}N_4 \cdot 2H_2O$: C, 68.55; H, 6.33; N, 16.00. Found: C, 68.15; H, 6.29; N, 15.91.

(2) Preparation and Characterization of Crystalline Copper Complexes. Crystalline complexes were prepared by slow evaporation in air of $CH_3OH/HOCH_2CH_2OH$ solutions containing 2:1 molar ratios of ligand: $Cu(ClO_4)_2$-$6H_2O$. Addition of ethylene glycol prevented the solutions from climbing the beaker walls and facilitated the formation of well-formed single crystals. In a typical preparation, a clear yellow solution containing 0.164 g (0.5 mmol) of **7b**, 0.0925 g (0.25 mmol) of $Cu(ClO_4)_2$-$6H_2O$, 35 mL of CH_3OH, and 2 mL of $HOCH_2CH_2OH$ was filtered through a fine frit and allowed to evaporate at room temperature. Complex **2** deposited as well-formed rectangular brown prisms. Anal. Calcd for **1**, $CuL_2(ClO_4)_2 \cdot 4CH_3OH$, $CuCl_2C_{46}H_{56}N_8O_{12}$: Cu, 6.06; C, 52.75; H, 5.39; N, 10.70; Cl, 6.77. Calcd for **1**, $CuL_2(ClO_4)_2 \cdot 5CH_3OH$, $CuCl_2C_{47}H_{60}N_8O_{13}$: Cu, 5.88; C, 52.30; H, 5.60; N, 10.38; Cl, 6.57. Found: Cu, 5.75; C, 52.20; H, 5.32; N, 10.20; Cl, 6.10. Anal. Calcd for **2**, $CuL'_2(ClO_4)_2 \cdot 5CH_3OH$, $CuCl_2C_{45}H_{58}N_8S_2O_{13}$: Cu, 5.48; C, 48.36; N, 10.03; H, 5.23. Calcd for **2**, $CuL'_2(ClO_4)_2 \cdot 3CH_3OH \cdot 2H_2O$, $CuCl_2C_{43}H_{52}N_8S_2O_{13}$: Cu, 5.84; C, 47.49; N, 10.30; H, 4.82. Found: Cu, 5.48; C, 46.2; N, 9.57; H, 4.78.

Crystals of complexes **1**–**4** were not stable in the absence of mother liquor. When the crystals were exposed to air and most solvents, the crystals cracked and became opaque, presumably due to loss of lattice CH_3OH. As a consequence, accurate determination of the number of lattice species by the usual combination of elemental analysis (Galbraith), unit cell parameter and density determination, and single-crystal X-ray structure determination was difficult. As an example of the difficulties encountered, crystals of **1** and **2**, even in CH_3OH/CCl_4 mixtures, rapidly lost CH_3OH, and densities measured by flotation gave values which were erroneously high. Use of the gradient method reduced the time required for density measurements to ~20 s and improved the values obtained; however, even with this technique, precise densities could not be determined (Table I).

For complex **1**, four ordered CH_3OH molecules per Cu were located crystallographically (vide infra) and, since the structure appears to contain no cavities large enough to hold additional lattice species, we have formulated **1** as the tetramethanolate. Complex **2**, which yielded three disordered CH_3OH molecules and two ordered O atoms per Cu, has been tentatively formulated with five CH_3OH lattice species per Cu rather than three CH_3OH and two H_2O (from $Cu(ClO_4)_2 \cdot 6H_2O$ or moist air), since the former composition shows greater consistency both with the observed density and the elemental analyses.

(3) Electronic Spectral Measurements. Electronic spectra were measured with a Cary 17 spectrophotometer that was interfaced with a

Table II. Fractional Atomic Coordinates and Thermal Parameters ($\times 10^3$) for **1**

	x	y	z	β_{11}[a]	β_{22}	β_{33}	β_{12}	β_{13}	β_{23}
Cu	0.0	0.0	0.0	6.6 (1)	3.65 (8)	15.0 (2)	0.05 (7)	0.2 (1)	1.3 (1)
N(1A)	0.0247 (5)	−0.1503 (4)	−0.0261 (7)	7.2 (5)	3.9 (3)	14.5 (11)	−0.2 (3)	−0.6 (6)	1.1 (5)
N(1B)	0.1808 (5)	0.0163 (4)	0.0881 (7)	6.2 (5)	4.3 (4)	15.6 (11)	−0.3 (3)	1.0 (6)	1.9 (5)
N(2A)	0.1115 (5)	−0.2960 (4)	0.0130 (7)	7.9 (6)	3.9 (3)	14.1 (10)	−0.3 (3)	0.4 (6)	2.3 (5)
N(2B)	0.3715 (5)	−0.0157 (4)	0.2089 (6)	7.3 (5)	4.5 (4)	11.7 (9)	−0.2 (3)	−0.2 (6)	1.3 (5)
C(1)	0.1997 (6)	−0.1282 (5)	0.2185 (8)	9.1 (7)	4.7 (4)	11.4 (11)	−0.6 (4)	−1.1 (7)	1.5 (6)
C(2)	0.1186 (8)	−0.0802 (6)	0.3371 (9)	13.4 (9)	6.7 (6)	13.8 (14)	−2.4 (6)	3.2 (9)	0.6 (7)
C(3)	0.3043 (7)	−0.1949 (6)	0.2907 (9)	10.8 (8)	5.7 (5)	17.3 (14)	−0.8 (5)	−2.7 (8)	4.0 (7)
C(1A)	0.1137 (6)	−0.1924 (5)	0.0681 (8)	7.4 (6)	3.9 (4)	13.3 (12)	−0.2 (4)	1.1 (7)	1.8 (6)
C(1B)	0.2511 (6)	−0.0437 (5)	0.1718 (8)	6.4 (6)	3.8 (4)	11.5 (11)	−0.4 (4)	−0.2 (6)	0.9 (5)
C(2A)	−0.0361 (6)	−0.2315 (5)	−0.1481 (8)	7.8 (7)	4.8 (5)	14.0 (13)	−0.9 (4)	−0.8 (7)	0.5 (6)
C(2B)	0.2599 (6)	0.0834 (5)	0.0693 (8)	7.7 (7)	4.8 (4)	14.4 (13)	−0.1 (4)	2.1 (7)	2.5 (6)
C(3A)	0.0163 (6)	−0.3221 (5)	−0.1250 (8)	8.1 (7)	4.1 (4)	13.2 (12)	−0.8 (4)	1.3 (7)	1.3 (6)
C(3B)	0.3794 (6)	0.0657 (5)	0.1463 (8)	7.1 (7)	4.9 (4)	11.1 (12)	−0.6 (4)	1.3 (7)	0.5 (6)
C(4A)	−0.0141 (7)	−0.4288 (5)	−0.2218 (8)	10.3 (8)	4.5 (4)	13.4 (12)	−1.7 (5)	2.2 (8)	1.3 (6)
C(4B)	0.4957 (6)	0.1178 (5)	0.1633 (8)	8.2 (7)	5.4 (5)	11.7 (12)	−0.5 (4)	2.2 (7)	0.4 (6)
C(5A)	−0.1121 (8)	−0.4472 (7)	−0.3558 (12)	11.9 (10)	7.1 (6)	27 (2)	−1.3 (6)	−0.2 (11)	−1.5 (9)
C(5B)	0.4913 (7)	0.2021 (7)	0.1005 (11)	9.6 (9)	8.8 (7)	27 (2)	−1.3 (6)	2.8 (10)	6.1 (10)
C(6A)	−0.1418 (10)	−0.5463 (8)	−0.4486 (13)	16.9 (13)	7.7 (7)	30 (2)	−3.4 (8)	−0.6 (13)	−3.6 (11)
C(6B)	0.5992 (9)	0.2552 (7)	0.1188 (13)	12.2 (11)	9.1 (7)	33 (2)	−1.9 (7)	6.4 (13)	7.4 (11)
C(7A)	−0.1742 (11)	−0.6286 (7)	−0.4109 (12)	22 (2)	6.4 (7)	21 (2)	−4.8 (8)	5.9 (14)	−1.0 (9)
C(7B)	0.7121 (8)	0.2241 (7)	0.1998 (11)	10.1 (9)	10.3 (8)	19 (2)	−3.7 (7)	3.7 (10)	0.8 (9)
C(8A)	0.0162 (12)	−0.6129 (7)	−0.2783 (15)	26 (2)	4.9 (6)	33 (3)	−0.8 (8)	−2 (2)	1.0 (10)
C(8B)	0.7184 (7)	0.1384 (7)	0.2555 (10)	8.2 (8)	11.0 (8)	18 (2)	−1.9 (6)	1.6 (9)	3.1 (9)
C(9A)	0.0459 (10)	−0.5124 (7)	−0.1816 (12)	21.0 (15)	5.3 (6)	27 (2)	−0.2 (7)	−4.9 (13)	1.1 (9)
C(9B)	0.6109 (7)	0.0851 (6)	0.2362 (9)	8.3 (7)	7.9 (6)	15.4 (13)	−1.1 (5)	1.4 (8)	2.8 (7)
Cl	0.6967 (2)	−0.1769 (2)	0.3802 (3)	16.2 (3)	7.4 (2)	19.1 (4)	1.0 (2)	−3.0 (3)	1.6 (2)
O(1)	0.6002 (6)	−0.1017 (5)	0.4112 (8)	14.7 (8)	10.9 (6)	30 (2)	3.3 (5)	1.4 (8)	7.1 (7)
O(2)	0.7630 (9)	−0.1930 (7)	0.5202 (10)	34 (2)	20.6 (10)	28 (2)	13.5 (10)	−4.8 (13)	8.4 (11)
O(3)	0.7806 (8)	−0.1380 (7)	0.3111 (12)	21.6 (12)	18.1 (10)	51 (3)	1.0 (8)	16.1 (15)	8.6 (13)
O(4)	0.6418 (10)	−0.2646 (7)	0.2719 (11)	36 (2)	12.5 (8)	37 (2)	−5.7 (9)	4.4 (15)	−6.7 (10)
O(1M)	0.3085 (6)	−0.4393 (4)	0.1086 (8)	17.1 (8)	6.6 (4)	30.5 (15)	2.9 (5)	−2.2 (9)	1.4 (6)
O(2M)	0.5125 (8)	−0.4033 (7)	0.3616 (11)	24.9 (13)	17.9 (10)	32 (2)	−0.7 (8)	−1.0 (12)	2.0 (11)

	x	y	z	β, Å^2		x	y	z	β, Å^2
C(1M)	0.336 (2)	−0.540 (2)	0.051 (2)	15.8 (6)	C(2M)	0.510 (2)	−0.3665 (13)	0.523 (2)	13.1 (5)

[a] The form of the anisotropic thermal ellipsoid is $\exp[-(\beta_{11}h^2 + \beta_{22}k^2 + \beta_{33}l^2 + 2\beta_{12}hk + 2\beta_{13}hl + 2\beta_{23}kl)]$.

Tektronix 4052 computer. Solutions of complexes **1**–**4** in CH_3OH appeared to be stable indefinitely at room temperature. Complex **2** did not exhibit the redox instability reported for other Cu(II)–thioether systems[15] and could be recrystallized unchanged from boiling CH_3OH. Spectra of the crystalline complexes were recorded as mineral oil mulls between quartz plates. The mineral oil coating appeared to preserve the complexes from the deterioration noted above.

(4) Magnetic Measurements. Magnetic susceptibility measurements were made on complexes **1** and **2** at 25 °C by using the Faraday technique. The apparatus was calibrated with $Ni(en)_3S_2O_3$. Crystals of the complexes were collected by filtration, washed quickly with CH_3OH, and air-dried for ~30 s. Care was taken to ensure that the crystals were dry but not to the point of opacity. The crystals were rapidly loaded into capsules which were then sealed for the magnetic measurements. Diamagnetic corrections of -554×10^{-6} and -526×10^{-6} cgs were calculated per Cu(II) from Pascal's constants[16] and applied to the susceptibilities of **1** and **2**, respectively. EPR spectra were recorded on a Varian E-12 spectrometer (X-band) calibrated with a Hewlett-Packard Model 5245L frequency counter and a Mn(II) standard. High-resolution spectra were obtained by cooling ~5 mM methanolic solutions of the complexes to 80 K. Relatively broad spectra of the polycrystalline complexes also were measured at 298 and 80 K.

(5) X-ray Diffraction Studies. Crystals of **1** and **2** were removed from mother liquor with a fine-glass fiber and transferred rapidly to a glass capillary which already contained some mother liquor. The crystals were immobilized with quick setting epoxy glue at a location well removed from the mother liquor. The open ends of the capillaries were then sealed with epoxy. Crystals of **1**, mounted in this fashion, showed a decay in the standard intensities of approximately 10% during the data collection period; crystals of **2** showed a random variation of ±6% with no appreciable decay. Crystal data and additional details of the data collection and refinement for both complexes are presented in Table I.

Complex 1. Intensity data were collected and corrected for decay, *Lp* effects, and absorption as described previously.[6] Diffractometer examination of the reciprocal lattice revealed no systematic absences.

The structure was solved by direct methods[17] and refined successfully in space group $P\bar{1}$ by using full-matrix least-squares techniques. Neutral atom scattering factors were used,[18] and anomalous dispersion corrections[19] were applied to the Cu and Cl atoms. An *E* map, calculated by using 222 phases from the starting set with the highest combined figure of merit, revealed the Cu and Cl atoms, along with portions of the ligand. The remaining nonhydrogen atoms, including two unique lattice CH_3OH molecules, were located on subsequent difference Fourier maps. Several cycles of isotropic unit weight refinement led to convergence with R_F = 0.142.

Hydrogen atoms were added to the model at calculated positions, with N–H and C–H bond lengths taken to be 0.87 and 0.95 Å, respectively.[20] A planar geometry was assumed for the amine N and aromatic C atoms, while methylene and methyl C atoms were assumed to be tetrahedral. Methyl H atoms were located by rotating at 5° intervals the idealized tetrahedral positions and computing the electron density at these positions. The orientation with the highest combined electron density was used. All H atoms, except those of CH_3OH, which we were unable to locate, were positioned in regions of positive electron density on a difference electron density map. H atoms were assigned temperature factors according to $B_H = B_n + 1$, where n is the atom bonded to H. Hydrogen atom parameters were not refined.

Additional refinement, using isotropic thermal parameters for methanol C atoms and anisotropic thermal parameters for all remaining

(15) Musker, W. K.; Olmstead, M. M.; Kessler, R. M.; Murphey, M. M.; Neagley, C. H.; Roush, P. B.; Hill, N. L.; Wolford, T. L.; Hope, H.; Delker, G.; Swanson, K.; Gorewit, B. V. *J. Am. Chem. Soc.* **1980**, *102*, 1225–26.

(16) Earnshaw, A. "Introduction to Magnetochemistry"; Academic Press: New York, 1968; pp 4–8.

(17) In addition to local programs for the IBM 360/70 computer, local modifications of the following programs were employed: Coppens' ABSORB program; Zalkin's FORDAP Fourier program; Johnson's ORTEP II thermal ellipsoid plotting program; Busing, Martin, and Levy's ORFEE error function program; Main, Lessinger, Declercq, Woolfson, and Germain's MULTAN 78 program for the automatic solution of crystal structures; and the FLINUS least-squares program obtained from Brookhaven National Laboratories.

(18) Cromer, D. T.; Waber, J. T. *Acta Crystallogr.* **1965**, *18*, 104–9.

(19) "International Tables for X-ray Crystallography"; Kynoch Press: Birmingham, England, 1962; Vol. III, pp 201–13.

(20) Churchill, M. R. *Inorg. Chem.* **1973**, *12*, 1213–4.

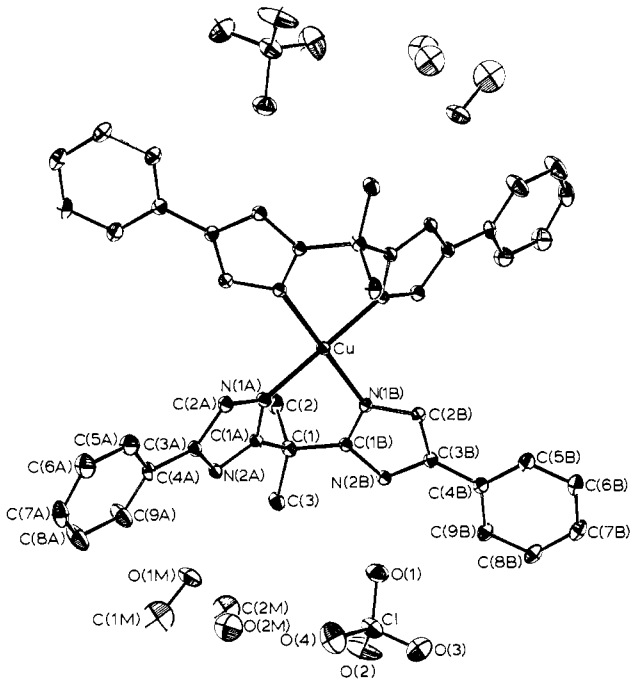

Figure 1. ORTEP view of complex **1** showing the atom numbering scheme.

nonhydrogen atoms, reduced R_F to 0.064 and R_{wF} to 0.067. For the final cycle, all parameter changes were within 0.2σ except for those of the CH_3OH atoms which were within 2.5σ, where σ is the esd obtained from the inverse matrix. A final difference map showed a general background of approximately ± 0.2 e/Å^3. The largest positive peaks (~ 0.84 e/Å^3) were residuals from a (possibly somewhat disordered) lattice CH_3OH species. Final atomic parameters are listed in Table II while views of the complex and its packing are given in Figures 1 and 2, respectively. Lists of observed and calculated structure factors and calculated H atom parameters are available.[21]

Complex 2. Intensity data were collected and corrected for decay, *Lp* effects, and absorption as described previously.[6] Weissenberg photographs and diffractometer examination of the reciprocal lattice revealed systematic absences for $h0l$, $l = 2n + 1$, and $0k0$, $k = 2n + 1$, fixing the space group as $P2_1/c$.

The structure was solved by the heavy-atom method and refined by using full-matrix least-squares techniques. Neutral atom scattering factors[18] were employed and anomalous dispersion corrections were applied to Cu, Cl, and S atoms.[19] Approximate Cu and S coordinates were determined from a Patterson map. Ligand and perchlorate atoms were located on several subsequent difference electron density maps and verified with the Patterson map. While vectors between the Cu and ligand atoms appeared with the expected weight, Cu–Cl vectors were too small. Attempts to refine the ClO_4 group led to unreasonable bond distances and angles, while on difference electron density maps, a large Cl residual persisted. Careful examination of a difference map, prepared by using phases derived from the Cu and ligand atoms after isotropic refinement, revealed that the perchlorate group was disordered. On the basis of bond distances and electron densities obtained from the difference map, a model consisting of two ClO_4 groups sharing two O atoms (O(1) and O(2)) was chosen. From the difference map electron densities, occupancies of the disordered atoms (Cl(A), Cl(B), O(3A), O(3B), O(4A), O(4B)) were set at 0.5 and, because the temperature factors of the A and B atoms refined to similar values, these atom multipliers were not refined.

Difficulties in locating the lattice CH_3OH species were also encountered, possibly as a result of the ClO_4 disorder and thermal motion. Seven possible sites for methanol C and O atoms were identified on the appropriate difference map; of these, three pairs (C(2M), O(2M); C(3M), O(3M); C(4M), O(4M)) showed interatomic distances approximating that expected for a methanol molecule. Each of these pairs showed unusually close contacts with *one* perchlorate group and gave unreasonably large isotropic temperature factors when allowed to refine at full occupancy. Consequently, these atoms were added to the model with atom multipliers of 0.5. The remaining atom (O(1M)) showed no unusually short interatomic contacts and refined smoothly at full occupancy. Attempts to locate a C atom bonded to O(1M) were unsuccessful. For these lattice species, O atoms were distinguished from C atoms on the basis of potential hydrogen bonding contacts to the perchlorate O atoms. Thus, the final model refined contains 1.5 CH_3OH molecules, one O atom, and one ClO_4 group per asymmetric unit.

Ligand H atoms were added to the model as described above and were not refined. No attempt was made to locate methanol H atoms. Several cycles of refinement with isotropic thermal parameters for the methanol atoms and anisotropic thermal parameters for the remaining nonhydrogen atoms reduced R_F to 0.089 and R_{wF} to 0.085. For the final cycle, all parameter changes were less than 0.2σ except those for methanol atoms which were less than 1.7σ, where σ is the esd obtained from the inverse matrix. A final difference map showed a general background of ± 0.3 e$^-$/Å^3; the largest positive peak was 0.52 e$^-$/Å^3. Final atomic parameters are listed in Table IV. Figures 3 and 4 show a view of the complex and its packing, respectively. Lists of observed and calculated structure factors and H atom parameters are available.[21]

(21) Supplementary material.

Table III. Selected Bond Distances (Å) and Angles (Deg) in **1**

Coordination Sphere			
Cu-N(1A)	1.979 (5)	Cu-N(1B)	1.960 (4)
Imidazole Rings			
N(1A)-C(1A)	1.326 (8)	N(2B)-C(1B)	1.345 (6)
N(1B)-C(1B)	1.329 (7)	N(2A)-C(3A)	1.389 (7)
N(1A)-C(2A)	1.391 (8)	N(2B)-C(3B)	1.382 (8)
N(1B)-C(2B)	1.375 (8)	C(2A)-C(3A)	1.356 (9)
N(2A)-C(1A)	1.348 (7)	C(2B)-C(3B)	1.363 (8)
Ligand			
C(1)-C(2)	1.55 (1)	C(1)-C(1B)	1.510 (9)
C(1)-C(3)	1.531 (9)	C(3A)-C(4A)	1.475 (8)
C(1)-C(1A)	1.522 (8)	C(3B)-C(4B)	1.467 (8)
Coordination Sphere			
N(1A)-Cu-N(1B)	88.1 (2)		
Imidazole Rings			
Cu-N(1A)-C(1A)	124.4 (4)	N(1B)-C(2B)-C(3B)	109.3 (6)
Cu-N(1B)-C(1B)	123.8 (4)	N(2A)-C(3A)-C(2A)	105.7 (5)
Cu-N(1A)-C(2A)	128.9 (4)	N(2B)-C(3B)-C(2B)	105.3 (5)
Cu-N(1B)-C(2B)	128.9 (4)	N(1A)-C(1A)-C(1)	122.4 (5)
C(1A)-N(1A)-C(2A)	106.5 (5)	N(1B)-C(1B)-C(1)	123.8 (5)
C(1B)-N(1B)-C(2B)	107.1 (5)	N(2A)-C(1A)-C(1)	127.3 (5)
C(1A)-N(2A)-C(3A)	108.3 (5)	N(2B)-C(1B)-C(1)	126.7 (5)
C(1B)-N(2B)-C(3B)	108.8 (5)	N(2A)-C(3A)-C(4A)	124.4 (6)
N(1A)-C(1A)-N(2A)	110.2 (5)	N(2B)-C(3B)-C(4B)	124.7 (6)
N(1B)-C(1B)-N(2B)	109.4 (5)	C(2A)-C(3A)-C(4A)	129.9 (6)
N(1A)-C(2A)-C(3A)	109.3 (6)	C(2B)-C(3B)-C(4B)	130.0 (6)
Ligand			
C(2)-C(1)-C(3)	110.3 (6)	C(3)-C(1)-C(1A)	111.1 (5)
C(2)-C(1)-C(1A)	107.4 (5)	C(3)-C(1)-C(1B)	111.6 (5)
C(2)-C(1)-C(1B)	109.7 (5)	C(1A)-C(1)-C(1B)	106.6 (5)

Results and Discussion

Description of the Structures. The structure of **1** consists of discrete $Cu^{II}L_2^{2+}$ (L = **7a**) cations with point symmetry $\bar{1}$ separated by perchlorate anions and lattice methanol molecules. The Cu atom exhibits planar equatorial N_4 coordination resulting from ligation by two centrosymmetrically related bidentate imidazole ligands. Apical ligation is not present. Both the ClO_4 groups and lattice methanol molecules are well removed from the Cu(II) centers with all O···Cu(II) distances greater than 4 Å. The CuN_4 unit is crystallographically required to be planar and has Cu–N distances (1.979 (5), 1.960 (4) Å, Table III) which are typical for tetrakis(imidazole)copper(II) complexes.[22-25] The N(1A)–Cu–N(1B) angle (88.1 (2)°) is typical for a Cu(II) complex of a bidentate nitrogen-donor ligand which forms a six-membered chelate ring.[26] In **1**, the chelate ring has adopted the high-energy

(22) Hori, F.; Kojima, Y.; Matsumoto, K.; Ooi, S.; Kuroya, H. *Bull. Chem. Soc. Jpn.* **1979**, *52*, 1076–79.
(23) Fransson, G.; Lundberg, B. K. S. *Acta Chem. Scand.* **1972**, *26*, 3969–76.
(24) Ivarsson, G. *Acta Chem. Scand.* **1973**, *27*, 3523–30.
(25) Akhtar, F.; Goodgame, D. M.L.; Goodgame, M.; Rayner-Canham, G. W.; Skapski, A. C. *J. Chem. Soc., Chem. Commun.* **1968**, 1389–90.
(26) Fawcett, T. G.; Rudich, S. M.; Toby, B. H.; Lalancette, R. A.; Potenza, J. A.; Schugar, H. J. *Inorg. Chem.* **1980**, *19*, 940–45.

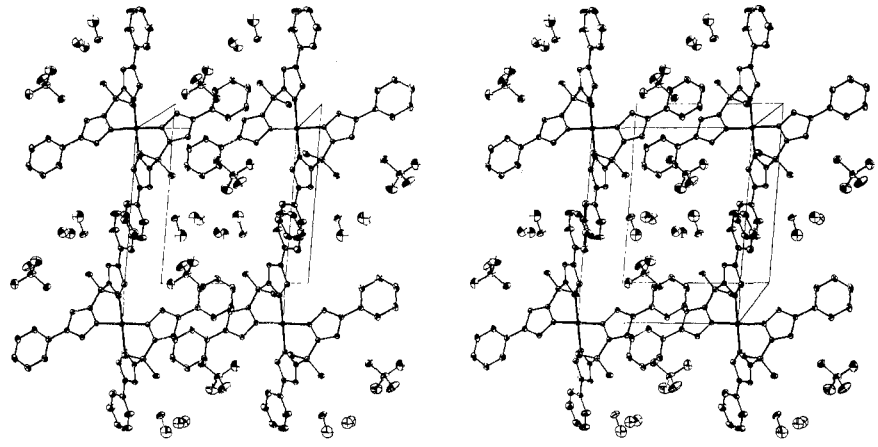

Figure 2. Stereoscopic packing diagram for **1** viewed approximately along *c* (pointed toward reader). The *a* axis is horizontal.

Table IV. Fractional Atomic Coordinates and Thermal Parameters ($\times 10^3$) for **2**

	x	*y*	*z*	β_{11}[a]	β_{22}	β_{33}	β_{12}	β_{13}	β_{23}
Cu	0.0	0.0	0.0	7.6 (1)	11.3 (2)	4.79 (6)	−1.3 (1)	1.25 (7)	−1.88 (10)
S	−0.0425 (2)	0.0145 (3)	−0.1494 (2)	11.1 (2)	22.6 (5)	5.1 (1)	−4.3 (3)	2.6 (1)	−4.5 (2)
N(1A)	−0.354 (6)	0.1640 (7)	−0.0125 (5)	8.5 (7)	10.9 (8)	4.5 (3)	−1.8 (6)	1.7 (4)	−1.1 (5)
N(1B)	−0.1646 (6)	−0.0333 (7)	−0.0156 (4)	6.9 (6)	12.6 (9)	4.7 (3)	−1.3 (6)	1.4 (4)	−2.2 (4)
N(2A)	−0.0925 (7)	0.3182 (9)	−0.0645 (5)	10.7 (8)	16.5 (11)	4.0 (4)	1.1 (8)	0.8 (4)	0.7 (5)
N(2B)	−0.3267 (7)	−0.0774 (8)	−0.0686 (5)	8.5 (7)	15.3 (10)	5.9 (4)	−2.2 (7)	0.4 (4)	−2.5 (5)
C(A)	−0.0475 (9)	0.1636 (11)	−0.1453 (5)	15.0 (12)	20 (2)	3.7 (4)	4.4 (11)	0.4 (5)	−1.7 (6)
C(B)	−0.1879 (10)	−0.019 (2)	−0.1475 (6)	12.2 (11)	46 (3)	4.8 (5)	−11 (2)	1.9 (6)	−5.7 (11)
C(1A)	−0.0579 (8)	0.2115 (11)	−0.0752 (6)	9.4 (9)	15.9 (14)	3.4 (4)	0.3 (9)	0.4 (5)	−0.2 (6)
C(1B)	−0.2237 (9)	−0.0418 (10)	−0.0771 (6)	8.3 (9)	20 (2)	4.7 (4)	−3.2 (9)	1.5 (5)	−3.4 (6)
C(2A)	−0.0541 (8)	0.2408 (9)	0.0396 (5)	10.3 (9)	10.5 (10)	4.0 (4)	−1.4 (8)	1.6 (5)	−0.2 (5)
C(2B)	−0.2328 (7)	−0.0647 (8)	0.0347 (5)	7.8 (8)	8.6 (8)	5.4 (4)	0.7 (7)	0.3 (5)	0.0 (5)
C(3A)	−0.0903 (7)	0.3383 (10)	0.0077 (5)	7.9 (8)	13.6 (12)	4.1 (4)	−1.7 (8)	1.2 (4)	0.8 (6)
C(3B)	−0.3356 (7)	−0.0916 (8)	0.0025 (6)	7.1 (8)	9.1 (9)	5.9 (5)	0.3 (7)	0.0 (5)	−0.3 (5)
C(4A)	−0.1262 (8)	0.4431 (9)	0.0374 (6)	10.8 (9)	9.4 (9)	4.2 (4)	−1.9 (8)	1.7 (5)	−0.2 (5)
C(4B)	−0.4365 (8)	−0.1353 (9)	0.0310 (7)	6.8 (8)	9.8 (10)	6.8 (5)	0.4 (7)	0.1 (6)	1.7 (6)
C(5A)	−0.1045 (10)	0.4625 (9)	0.1092 (7)	17.0 (13)	10.0 (11)	5.1 (5)	−0.3 (9)	0.5 (6)	0.3 (6)
C(5B)	−0.4411 (10)	−0.1381 (12)	0.1023 (8)	10.8 (11)	21 (2)	7.9 (7)	−3.1 (11)	1.1 (7)	3.1 (9)
C(6A)	−0.1381 (12)	0.5598 (12)	0.1389 (7)	23 (2)	11.7 (13)	5.5 (5)	−2.0 (13)	2.7 (8)	−1.1 (7)
C(6B)	−0.5317 (12)	−0.179 (2)	0.1302 (9)	10.7 (12)	32 (3)	9.0 (8)	−3.2 (15)	1.5 (8)	5.2 (12)
C(7A)	−0.1964 (12)	0.6393 (10)	0.0966 (9)	21 (2)	8.9 (11)	8.0 (7)	1.7 (11)	1.4 (9)	0.6 (8)
C(7B)	−0.6218 (12)	−0.2159 (14)	0.0882 (11)	10.8 (13)	21 (2)	10.5 (9)	2.7 (12)	1.2 (10)	5.4 (12)
C(8A)	−0.2142 (12)	0.6200 (11)	0.0245 (9)	21 (2)	11.3 (13)	7.0 (7)	2.4 (12)	−0.3 (9)	0.5 (8)
C(8B)	−0.6192 (10)	−0.2124 (13)	0.0179 (10)	8.7 (11)	20 (2)	10.1 (9)	−3.6 (11)	−0.1 (8)	0.8 (11)
C(9A)	−0.1813 (10)	0.5228 (10)	−0.0040 (6)	15.5 (12)	11.8 (12)	5.4 (5)	1.4 (10)	−0.4 (6)	1.1 (6)
C(9B)	−0.5275 (9)	−0.1728 (11)	−0.0111 (7)	9.9 (11)	15.5 (13)	8.6 (7)	−3.2 (10)	0.9 (7)	−0.8 (8)
Cl(A)[b]	−0.2049 (8)	0.6975 (8)	−0.2213 (4)	18.8 (10)	13.9 (9)	5.7 (3)	1.0 (8)	0.0 (4)	2.2 (4)
Cl(B)[b]	−0.1898 (8)	0.6054 (10)	−0.2114 (5)	16.6 (9)	17.7 (11)	5.9 (4)	4.3 (8)	0.5 (4)	0.8 (5)
O(1)	−0.1965 (9)	0.6083 (11)	−0.2810 (6)	25.6 (15)	28 (2)	7.4 (5)	4.1 (13)	2.2 (7)	2.7 (8)
O(2)	−0.251 (2)	0.647 (2)	−0.1705 (10)	53 (4)	34 (3)	16.4 (11)	7 (2)	19 (2)	7.5 (15)
O(3A)[b]	−0.290 (2)	0.763 (2)	−0.2505 (12)	19 (2)	27 (3)	9.1 (11)	8 (2)	−3.9 (13)	−0.3 (15)
O(3B)[b]	−0.158 (2)	0.500 (2)	−0.1829 (10)	27 (3)	21 (3)	6.9 (9)	4 (3)	−1.6 (12)	1.7 (14)
O(4A)[b]	−0.107 (3)	0.770 (3)	−0.208 (2)	25 (4)	25 (4)	12.3 (15)	−9 (4)	−2 (2)	4 (2)
O(4B)[b]	−0.100 (3)	0.686 (3)	−0.196 (2)	24 (4)	22 (4)	17 (3)	1 (4)	−10 (3)	−2 (3)

	x	*y*	*z*	*B*, Å^2		*x*	*y*	*z*	*B*, Å^2
O(1M)	−0.4641 (11)	0.8724 (12)	−0.1997 (7)	17.9 (4)	C(2M)[b]	−0.290 (3)	0.223 (3)	−0.271 (2)	11.6 (9)
O(2M)[b]	−0.267 (3)	0.301 (3)	−0.301 (2)	17 (1)	C(3M)[b]	−0.526 (3)	−0.466 (3)	−0.109 (2)	15 (1)
O(3M)[b]	−0.512 (3)	−0.441 (4)	−0.165 (2)	25 (1)	C(4M)[b]	−0.192 (4)	0.340 (4)	−0.279 (2)	15 (1)
O(4M)[b]	−0.186 (2)	0.386 (2)	−0.2038 (13)	12.2 (6)					

[a] See footnote in Table II. [b] For these atoms, the atom multiplier equals 0.5. See text for discussion.

boat conformation[26] with displacements in the same direction of Cu and C(1) [0.618 and 0.584 Å, respectively] from the plane defined by N(1A), N(1B), C(1A), and C(1B) (plane V, Table VI).

Both crystallographically unique imidazole and phenyl groups are planar to within 0.03 Å (planes I–IV, Table VI). Moreover, the individual phenylimidazole units are nearly coplanar as indicated by the dihedral angles of 1.3 and 4.2° between each imidazole group and the phenyl ring directly attached to it. Dihedral angles between the planes of the imidazole groups and the planar CuN_4 unit are 34.0 and 34.3°. Bond distances and angles within the chelating ligand are typical for their type, and, excluding the phenyl rings, corresponding bond distances for the A and B halves of the ligand are equivalent within experimental error. The phenyl rings show typical bond distances (range 1.32 (1)–1.41 (1) Å, average 1.37 (2) Å) and angles (range 116.7 (6)–123.0 (7)°, average 120.3 (15)°).

The perchlorate ions appear to be loosely held in lattice holes by Coulombic forces and weak hydrogen bonds to methanol hydroxyl and imidazole N–H groups. Individual perchlorate bond distances (range 1.353 (7)–1.440 (8) Å) and angles (range 107.9 (6)–113.7 (6)°) are within a few standard deviations of those expected while the average Cl–O distance (1.40 (4) Å) is within 0.02 Å of those reported for similar structures.[27] The average

Table V. Selected Bond Distances (Å) and Angles (Deg) in 2

	Coordination Sphere		
Cu-S	2.824 (5)	Cu-N(1B)	2.019 (7)
Cu-N(1A)	2.020 (9)		
	Imidazole Rings		
N(1A)-C(1A)	1.32 (1)	N(2B)-C(1B)	1.34 (1)
N(1B)-C(1B)	1.30 (1)	N(2A)-C(3A)	1.39 (1)
N(1A)-C(2A)	1.38 (1)	N(2B)-C(3B)	1.37 (1)
N(1B)-C(2B)	1.38 (1)	C(2A)-C(3A)	1.37 (1)
N(2A)-C(1A)	1.37 (1)	C(2B)-C(3B)	1.36 (1)
	Ligand		
S-C(A)	1.79 (1)	C(B)-C(1B)	1.47 (2)
S-C(B)	1.81 (1)	C(3A)-C(4A)	1.46 (1)
C(A)-C(1A)	1.46 (1)	C(3B)-C(4B)	1.48 (1)
	Coordination Sphere		
S-Cu-N(1A)	79.0 (3)	N(1A)-Cu-N(1B)	89.0 (3)
S-Cu-N(1B)	78.2 (2)		
	Imidazole Rings		
Cu-N(1A)-C(1A)	123.1 (8)	N(1B)-C(2B)-C(3B)	109.8 (9)
Cu-N(1B)-C(1B)	125.7 (7)	N(2A)-C(3A)-C(2A)	105 (1)
Cu-N(1A)-C(2A)	127.7 (7)	N(2B)-C(3B)-C(2B)	104.2 (9)
Cu-N(1B)-C(2B)	127.3 (7)	N(1A)-C(1A)-C(A)	124 (1)
C(1A)-N(1A)-C(2A)	108.7 (9)	N(1B)-C(1B)-C(B)	127.5 (9)
C(1B)-N(1B)-C(2B)	106.6 (8)	N(2A)-C(1A)-C(A)	124 (1)
C(1A)-N(2A)-C(3A)	109.6 (9)	N(2B)-C(1B)-C(B)	122 (1)
C(1B)-N(2B)-C(3B)	109.2 (9)	N(2A)-C(3A)-C(4A)	124 (1)
N(1A)-C(1A)-N(2A)	107.9 (9)	N(2B)-C(3B)-C(4B)	123.8 (9)
N(1B)-C(1B)-N(2B)	110.1 (9)	C(2A)-C(3A)-C(4A)	131 (1)
N(1A)-C(2A)-C(3A)	108.8 (9)	C(2B)-C(3B)-C(4B)	132 (1)
	Ligand		
Cu-S-C(A)	91.3 (4)	S-C(A)-C(1A)	115.9 (9)
Cu-S-C(B)	92.2 (4)	S-C(B)-C(1B)	116.2 (8)
C(A)-S-C(B)	100.7 (8)		

Table VI. Deviations from Least-Squares Planes (Å) and Dihedral Angles (Deg) for 1

	I		
N(1A)[a]	0.004	C(2A)[a]	−0.003
N(2A)[a]	0.001	C(3A)[a]	0.002
C(1A)[a]	−0.003		
	II		
N(1B)[a]	0.008	C(2B)[a]	−0.009
N(2B)[a]	−0.002	C(3B)[a]	0.007
C(1B)[a]	−0.003		
	III		
C(4A)[a]	−0.029	C(7A)[a]	−0.036
C(5A)[a]	0.010	C(8A)[a]	0.006
C(6A)[a]	0.017	C(9A)[a]	0.021
	IV		
C(4B)[a]	0.025	C(7B)[a]	0.021
C(5B)[a]	−0.011	C(8B)[a]	−0.007
C(6B)[a]	−0.012	C(9B)[a]	−0.016
	V		
Cu	0.618	C(1)	0.584
N(1A)[a]	0.007	C(1A)[a]	−0.008
N(1B)[a]	−0.007	C(1B)[a]	0.008
	Dihedral Angles[b]		
I, II	51.8	II, IV	4.2
I, III	1.3		

[a] Atoms used to define plane. [b] The CuN_4 unit is strictly coplanar. Dihedral angles between this plane and planes I and II are 34.0 and 34.3°, respectively.

O–Cl–O angle (110 (2)°) is, within experimental error, equal to the tetrahedral value.

The structure of **2** consists of discrete $Cu^{II}L'_2{}^{2+}$ (L' = **7b**) cations of point symmetry $\bar{1}$ separated by perchlorate anions and lattice methanol molecules. Each Cu atom exhibits tetragonal N_4S_2 coordination arising from ligation by two centrosymmetrically related tridentate N_2S-donor ligands. The imidazole N donors occupy equatorial positions while the thioether S atoms are apical. The CuN_4 unit is planar (crystallographically required) and shows Cu–N bond lengths (2.020 (9), 2.019 (7) Å, Table V) which lie in the range reported for other tetrakis(imidazole)copper(II) complexes.[22-25] The N(1A)–Cu–N(1B) angle (89.0 (3)°) is typical for bonding of this type and compares well with the corresponding value of 88.1 (2)° observed for **1**.

The Cu–S bond length is 2.824 (5) Å, and is the second example of an apical Cu(II)–thioether bond. A Cu–thioether bond of similar length has been reported for plastocyanin.[4] The only other known examples of apical Cu(II)–S interactions are those of apical Cu(II)–thiourea (2.943 (1), 2.927 (1) Å)[28] and apical Cu(II)–disulfide (3.057 (10), 3.138 (9) Å;[29a] 3.16 (1), 3.28 (1) Å[29b]). Equatorial Cu(II)–thioether ligation yields bond lengths in the range 2.3–2.45 Å.[27,30] Due to the limited bite of the tridentate ligand, the Cu–S bond is tilted. The S–Cu–N(1A) and S–Cu–N(1B) angles of 79.0 (3) and 78.2 (2)°, respectively, show that the S donor in the bridge is tilted in the direction of the N donors from the attached imidazole groups.

As was observed for **1**, the imidazole and phenyl groups essentially are planar (planes I–IV, Table VII). Also, the individual phenylimidazole units are nearly coplanar with dihedral angles of 9.0 and 12.3° between each imidazole group and its directly attached phenyl ring. In contrast to **1**, the imidazole groups are nearly perpendicular to the planar CuN_4 unit as indicated by the imidazole/CuN_4 dihedral angles of 71.1 and 84.3°. These observations suggest that phenyl–imidazole coplanarity in **1** and **2**

Table VII. Deviations from Least-Squares Planes (Å) and Dihedral Angles (Deg) for 2

	I		
N(1A)[a]	−0.004	C(2A)[a]	0.002
N(2A)[a]	−0.002	C(3A)[a]	0.000
C(1A)[a]	0.004		
	II		
N(1B)[a]	0.001	C(2B)[a]	−0.005
N(2B)[a]	−0.005	C(3B)[a]	0.006
C(1B)[a]	0.003		
	III		
C(4A)[a]	0.007	C(7A)[a]	0.018
C(5A)[a]	−0.004	C(8A)[a]	−0.015
C(6A)[a]	−0.009	C(9A)[a]	0.007
	IV		
C(4B)[a]	0.005	C(7B)[a]	0.002
C(5B)[a]	−0.007	C(8B)[a]	−0.004
C(6B)[a]	0.004	C(9B)[a]	0.001
	V		
Cu[a]	−0.056	C(A)[a]	−0.126
S[a]	0.086	C(1A)[a]	0.067
N(1A)[a]	0.029		
	VI		
Cu[a]	−0.009	C(B)[a]	−0.026
S[a]	0.001	C(1B)[a]	0.010
N(1B)[a]	0.024		
	Dihedral Angles[b]		
I, II	89.1	II, IV	9.0
I, III	12.3		

[a] Atoms used to define plane. [b] The CuN_4 unit is strictly coplanar. Dihedral angles between this plane and planes I and II are 84.3 and 71.1°, respectively.

(27) Ou, C. C.; Miskowski, V. M.; Lalancette, R. A.; Potenza, J. A.; Schugar, H. J. *Inorg. Chem.* **1976**, 15, 3157–61.

(28) Belicci Ferrari, M.; Calzolari Capacchi, L.; Gasparri Fava, G.; Montenero, A.; Nardelli, M. *Kristallografiya* **1972**, *17*, 22–32.

(29) (a) Thich, J. A.; Mastropaolo, D.; Potenza, J. A.; Schugar, H. J. *J. Am. Chem. Soc.* **1974**, *96*, 726–31. (b) Miyoshi, K.; Sugiura, Y.; Ishizu, K.; Iitaka, Y.; Nakamura, H. *Ibid.* **1980**, *102*, 6130–36.

(30) Brubaker, G. R.; Brown, J. N.; Yoo, M. K.; Kinsey, R. A.; Kutchan, T. M.; Mottel, E. A. *Inorg. Chem.* **1979**, *18*, 299–302.

Table VIII. Summary of Electronic Spectral Results and Assignments

compd	soln (25 °C) $\bar{\nu}$, cm^{-1}	soln (25 °C) ϵ	mull (80 K) $\bar{\nu}$, cm^{-1}	assignt
ligand **7a**	38 200	55 000		phenyl, $\pi \rightarrow \pi^*$
complex **1**	49 000	138 000		ImH, $\pi \rightarrow \pi^*$ + n(ImH) → Cu(II)
	38 300	150 000		phenyl, $\pi \rightarrow \pi^*$
	25 600	205	25 700	π(ImH) → Cu(II)
	14 800	105	17 800 (sh)	LF
	12 500 (sh)	100	15 400	LF
ligand **7b**	49 800	47 200		ImH, $\pi \rightarrow \pi^*$ + thioether n → π^*[34]
	37 500	43 600		phenyl, $\pi \rightarrow \pi^*$
	25 600	16		trace Cu(II) contamination
complex **2**	48 800	60 000		ImH, $\pi \rightarrow \pi^*$ + n(ImH) → Cu(II)
	37 700	67 000		phenyl, $\pi \rightarrow \pi^*$
	27 800	244	26 700	π(ImH) → Cu(II)
	18 200	35	20 000	LF
	15 000	30	14 700	LF
ligand **7c**	43 500	25 000	41 600	ImH, $\pi \rightarrow \pi^*$ + thioether n → π^*[34]
complex **4**	48 100	68 000	45 400	ImH, $\pi \rightarrow \pi^*$ + n(ImH) → Cu(II)
	26 300 (sh)	200	26 200	π(ImH) → Cu(II)
	18 100	53	19 600	LF
	14 500	40	14 900	LF
ligand **7d**	37 500	33 800		phenyl, $\pi \rightarrow \pi^*$
complex **3**	49 500	130 000		ImH, $\pi \rightarrow \pi^*$ + n(ImH) → Cu(II)
	38 200	142 000	37 700	phenyl, $\pi \rightarrow \pi^*$
			34 400 (sh)	?
	25 600	260	26 600	π(ImH) → Cu(II)
	17 100	110	17 500	LF
			14 100 (sh)	LF

results either from electron delocalization between the imidazole and phenyl rings or from packing of adjacent molecules (Figures 2 and 4) rather than from interaction with the metal. Large CuN_4/ligand dihedral angles have been observed for Cu(imidazole)$_4$·2I[25] and Cu(pyrazole)$_4$Cl$_2$;[31] in the latter case, the large angle was attributed to hydrogen bonding between the pyrazole NH groups and the apical chloride ions. Both the nonpolar nature of the apical thioether groups and the position of NH in the imidazole ring argue against a similar explanation for **2**.

Bond distances and angles within the tridentate ligand are typical. For example, the C–S thioether linkages and C–S–C bond angle (1.79 (1), 1.81 (1) Å; 100.7 (8)°) compare favorably with the values reported for bis(β-(methylmercapto)ethylamine)copper(II) diperchlorate (1.799 (4), 1.806 (4) Å; 104.0 (2)°)[27] and (perchlorato)(1,8-bis(2-pyridyl)-3,6-dithiaoctane)copper(II) perchlorate (1.806 (8), 1.813 (12), 1.782 (12), 1.804 (8) Å; 100.9 (5), 102.3 (4)°),[30] both of which contain equatorial Cu(II)–thioether ligation. The phenyl rings also show typical bond distances (range 1.34 (2)–1.39 (2), average 1.365 (12) Å) and angles (range 117 (1)–123 (1)°, average 120 (2)°).

As in **1**, the perchlorate anions are held loosely in lattice holes. The perchlorate distances and angles, which span a rather large range (1.23 (2)–1.57 (2) Å; 95 (2)–130 (1)°) but which average (1.39 Å, 109°) close to the expected values,[27] are not unusual in the sense that comparable ranges have been reported for other structures[32] where disorder and/or thermal motion caused similar problems.

Electronic Structural Aspects of 1 and 2. Our characterization of **1** and **2** as Cu(II) complexes is in harmony with the results of magnetic susceptibility, ESR, and electronic spectral studies. The corrected magnetic moments of polycrystalline **1** and **2** at 298 K are 1.68 (5) and 1.64 (5) μ_B, respectively, and are representative of magnetically dilute Cu(II) complexes. ESR spectra of **1** and **2** are presented in Figures 5 and 6, respectively. Both spectra are characteristic of tetragonal Cu(II) chromophores. ESR spectra having similar appearance have been observed for planar Cu(II) chromophores having four pyrazole[8,9] and (probably) four guanosine ligands.[33] Thus, the solid-state structures of **1** and **2**

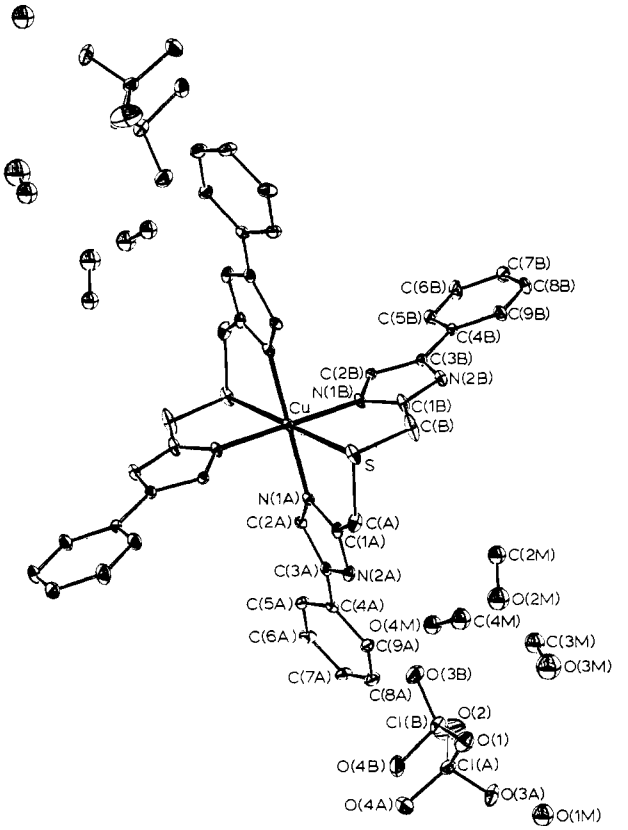

Figure 3. ORTEP view of complex **2** showing the atom numbering scheme.

appear to be maintained in CH_3OH solution. The approximately 10-line nitrogen hyperfine splitting on the $g_\parallel$ peaks arises from inequivalency of the four imidazole N donors. Detailed simulations of these spectra were not performed. Approximate ESR param-

(31) Mighell, A.; Santoro, A.; Prince, R.; Reimann, C. *Acta Crystallogr., Sect. B* **1975**, *B31*, 2479–82.

(32) Fawcett, T. G.; Fehskens, E. E.; Potenza, J. A.; Schugar, H. J.; Lalancette, R. A. *Acta Crystallogr., Sect. B* **1979**, *B35*, 1460–63 and references cited therein.

(33) Chao, Y.-Y. C.; Kearns, D. R. *J. Am. Chem. Soc.* **1977**, *99*, 6425–34.

(34) Several percent of this absorption band may arise from the (unresolved) n → π^* absorption expected for the alkyl thioether fragment. See: Passerini, R. C. In "Organic Sulfur Compounds"; Kharasch, N., Ed., Permagon Press: New York, 1961; pp 57–74.

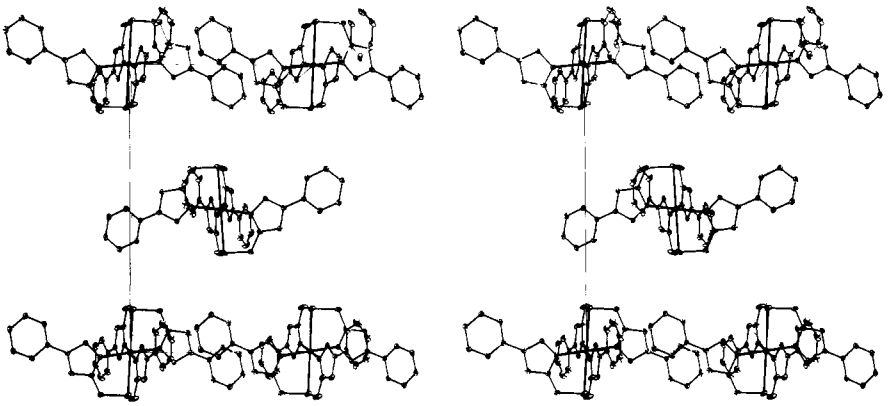

Figure 4. Stereoscopic packing diagram for **2** viewed approximately along $\bar{a}$. The b axis is horizontal. For clarity, perchlorate anions and lattice methanol molecules are not shown.

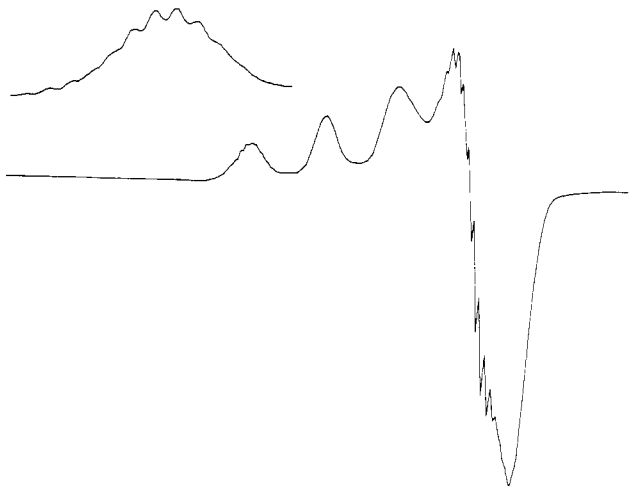

Figure 5. Low-temperature (80 K) X-band ESR spectra of **1** (~5 mM) in CH_3OH.

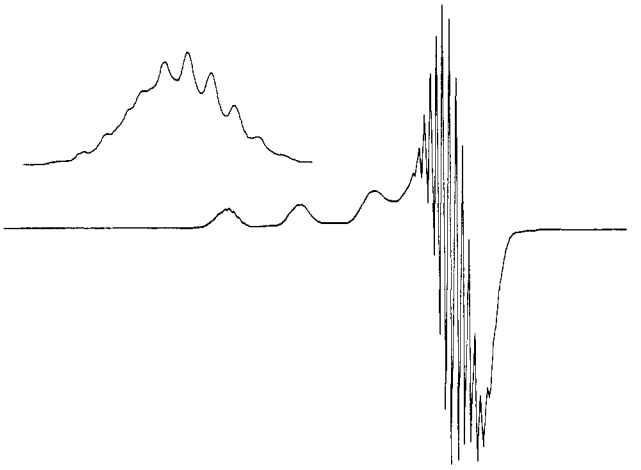

Figure 6. Low-temperature (80 K) X-band ESR spectra of **2** (~5 mM) in CH_3OH.

eters for **1** include $g_\perp = \sim 2.08$, $g_\parallel = \sim 2.26$, $A_\parallel^{Cu} = \sim 169$ G (~178 (10^4 cm^{-1})), and $A_\perp^{N} = \sim 12$ G and are similar to those reported for other CuN_4^{2+} chromophores.[8,33] Complex **2** yields ESR spectra of similar appearance whose approximate parameters are $g_\perp = \sim 2.07$, $g_\parallel = \sim 2.24$, $A_\parallel^{Cu} = \sim 183$ G (~191 (10^4 cm^{-1})), and $A_\perp^{N} = \sim 12$G. In view of the structure of the ligand in **2**, it is difficult to imagine how tetrakis-imidazolyl ligation could be maintained without simultaneous maintenance of apical Cu(II)–thioether bonding.

Also consistent with the ESR results are the solution and mull electronic spectra of complexes **1** and **2** (Figures 7 and 8). Electronic spectral results and assignments for the ligands and

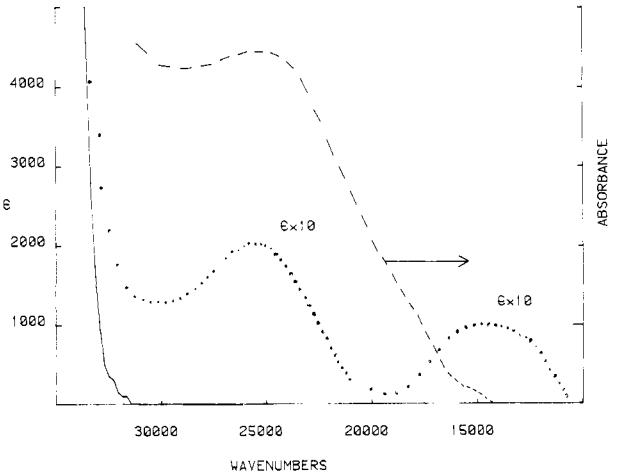

Figure 7. Electronic spectra of **1** at 80 K as a mineral oil mull (---) and at 25 °C as a 2 mM solution in CH_3OH (···). Solution spectra of the free ligand at 25 °C are indicated by the solid line.

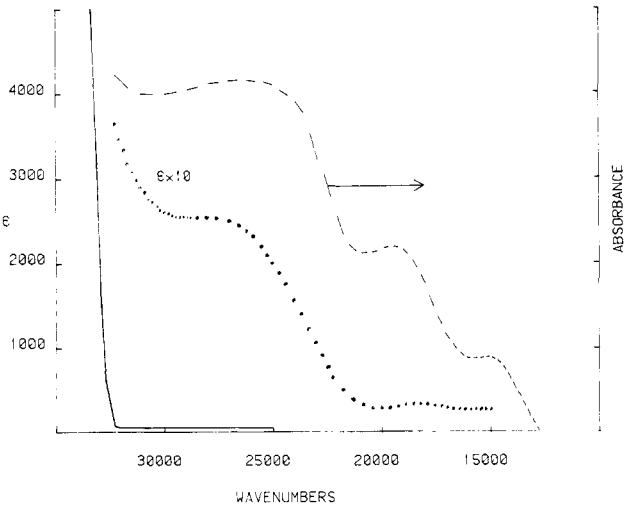

Figure 8. Electronic spectra of **2** at 80 K as a mineral oil mull (---) and at 25 °C as a 10 mM solution in CH_3OH (···). Solution spectra of the free ligand at 25 °C are indicated by the solid line.

complexes studied here are presented in Table VIII. Similarity between the solid-state and solution structures of **1** is implied by their common electronic absorptions at ~15 000 and ~26 000 cm^{-1}. The strong UV absorption beginning at ~33 000 cm^{-1} originates from the phenyl substituent; the lowest energy electronic absorption of imidazole and alkylimidazoles ($\pi \rightarrow \pi^*$) occurs at 40 000–45 000 cm^{-1}. We have described the electronic structure of tetragonal Cu(II)–imidazole chromophores elsewhere.[7,10] Ligand to metal charge-transfer (LMCT) absorptions in the

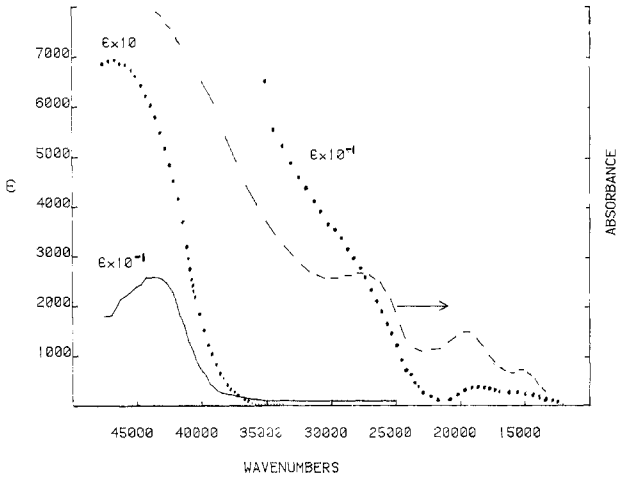

Figure 9. Electronic spectra of $CuL_2{\cdot}2ClO_4{\cdot}XCH_3OH$ where L = ligand **7c**. Mull spectra (80 K) and solution spectra (25 °C) in CH_3OH (10 mM) are given by the dashed and dotted lines, respectively. Solution spectra of the free ligand at 25 °C are indicated by the solid line.

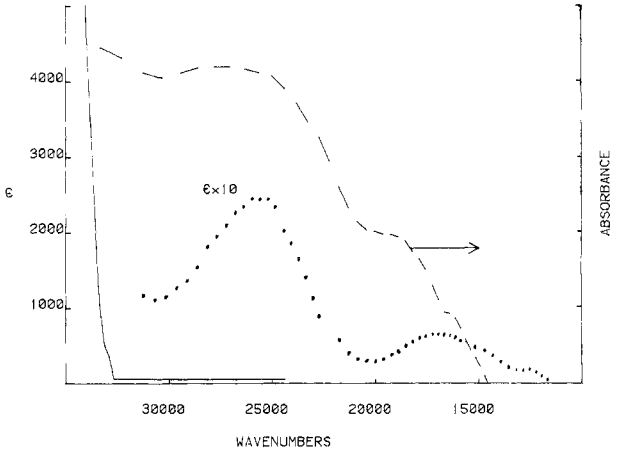

Figure 10. Electronic spectra of $CuL_2{\cdot}2ClO_4{\cdot}XCH_3OH$ where L = ligand **7d**. Mull spectra (80 K) and solution spectra (25 °C) in CH_3OH (2 mM) are given by the dashed and dotted lines, respectively. Solution spectra of the free ligand at 25 °C are indicated by the solid line.

near-UV and UV spectral regions originate from the N-donor lone pair (n) as well as from two π-symmetry ring orbitals. The n(ImH) → Cu(II) LMCT and imidazole $\pi \rightarrow \pi^*$ absorptions usually give rise to an unresolved combined absorption at ~ 40 000–45 000 cm^{-1}. The degree of resolution and intensity of the π(ImH) → Cu(II) LMCT absorptions depend upon the structure of the ligand. These absorptions appear as a poorly resolved shoulder at 32 300 cm^{-1} (ϵ = 340) in solution spectra of the tetrakis Cu(II) complex of unsubstituted imidazole. In contrast, the tetrakis complexes of Cu(II) with various 4,5-dialkylimidazoles exhibit well-resolved π(ligand) → Cu(II) LMCT absorptions at ~29 000 cm^{-1} (ϵ ~1500) and ~33 000 cm^{-1} (ϵ ~ 1500).[7] The new ligands described here all contain two 2,5-disubstituted imidazole units. Solution spectra of the corresponding Cu(II) complexes (Figures 7–10) all exhibit electronic absorption at ~26 000 cm^{-1} (ϵ = 200–260). In view of the position and intensity of this electronic transition, we assign it to poorly resolved π(ligand) → Cu(II) LMCT. Mull spectra (Figures 7–10) of complexes **1–4** reveal two absorptions in the 14 000–20 000-cm^{-1} region which undergo modest shifts in the corresponding methanolic solution spectra. The energies and intensities ($\epsilon \leq 110$) of these bands are appropriate for ligand field transitions of planar or tetragonal Cu(II) chromophores having equatorial CuN_4 ligation. Ligand field transitions at energies up to 20 600 cm^{-1} have been reported[35] for $CuL_2{\cdot}2ClO_4$ complexes (L = an alkylated ethylenediamine); LMCT in this energy region can be dismissed owing to the poorly reducing nature of such ligands. Thus, all absorptions of complexes **1–4** in the 14 000–28 000-cm^{-1} region reasonably may be assigned to ligand field and π(ImH) → Cu(II) LMCT transitions. Whereas equatorial thioether–Cu(II) bonding results in prominent ($\epsilon > 1000$) S* → Cu(II) LMCT at ~25 000 cm^{-1},[11,36] a corresponding absorption could not be detected for the apical thioether–Cu(II) bonding demonstrated for **2** and likely present in **4**. The electronic absorptions of the complexes with and without thioether ligation essentially were identical.

Thioether–Cu(II) LMCT in Plastocyanin. Our prior spectroscopic studies of model Cu(II)–thiolate[6] and Cu(II)–ImH chromophores[7] indicate that LMCT of these types undergoes an approximately 10 000 cm^{-1} red-shift when the Cu(II) geometry changes from planar or five-coordinate to pseudotetrahedral. Since a major portion of this shift must reflect the ligand field dependency of the Cu(II) d vacancy (i.e., the LMCT acceptor orbital), a comparable red-shift is expected for S* → Cu(II) LMCT. As noted above, various planar, tetragonal, and five-coordinate Cu(II) complexes having equatorial S*–Cu(II) bonding exhibit prominent ($\epsilon > 1000$) S* → Cu(II) LMCT at ~25 000 cm^{-1}.[11,36] If the S*–Cu bond in plastocyanin were of the equatorial type (~2.3 Å), this protein should exhibit prominent ($\epsilon > 1000$) S* → Cu(II) LMCT at ~15 000 cm^{-1} owing to the relatively small ligand field[5] developed by the N_2SS^* donor set. In view of the apical nature of the S*–Cu(II) bonding (~2.9 Å) reported for plastocyanin, this band should be relatively weak. While such an absorption could not be detected for our model tetragonal $CuN_4S^*S^*$ chromophore, we can not infer that S* → Cu(II) LMCT necessarily is undetectable for the highly distorted CuN_2SS^* protein chromophore.

Other workers have assigned a poorly resolved plastocyanin absorption at 18 100 cm^{-1} (ϵ = 1163, estimated by gaussian analysis) as S* → Cu(II) LMCT.[5] Unless the intensity of this band has been seriously overestimated, such an assignment is not supported by the subsequent protein crystallographic results and our study of model apical Cu–S* chromophores. In view of the spectroscopic similarities[5] of the type 1 proteins and the weakly ligating[37] nature of thioether donors, it is possible that apical S* → Cu(II) bonding obtains for all methionine-containing type 1 proteins. The significance of Cu(II)–thioether complexes as spectroscopic *models*[38] for the type 1 proteins seems to be overemphasized. Our skepticism[11,27] regarding the biological relevance of S* → Cu(II) bonding has been misinterpreted.[38] We have never dismissed the possibility of Cu(II)–methionine bonding (except for the methionine-free protein stellacyanin). However, we are not convinced that spectroscopic and other features of type 1 proteins depend in a profound way upon Cu(II)–methionine ligation.

Acknowledgment. This work was supported by the National Institutes of Health (Grant AM-16412 to H.J.S.) and the Rutgers Computing Center. We thank Professor Spencer Knapp for advice regarding the ligand syntheses, Mr. Steven Rudich for obtaining the ESR spectra, and Mr. Brian Toby for help in obtaining the X-ray diffraction data. We thank Professors Harry Gray, Ed Solomon, and David McMillen for helpful discussions.

Supplementary Material Available: Tables of hydrogen atom coordinates and thermal parameters and observed and calculated structure factors for **1** and **2** (24 pages). Ordering information is given on any current masthead page.

(35) Grenthe, I.; Paoletti, P.; Sandström, M.; Glikberg, S. *Inorg. Chem.* **1979**, *18*, 2687–92.
(36) Amundsen, A. R.; Whelan, J.; Bosnich, B. *J. Am. Chem. Soc.* **1977**, *99*, 6730–39.
(37) Sigel, H.; Scheller, K. H.; Rheinberger, V. M.; Fischer, B. E. *J. Chem. Soc., Dalton Trans.* **1980**, 1022–28.
(38) Ferris, N. S.; Woodruff, W. H.; Rozabacher, D. B.; Jones, T. E.; Ochrymowycz, L. A. *J. Am. Chem. Soc.* **1978**, *100*, 5939–42.